Journal of Aerosol Science 150 (2020) 105654

Contents lists available at ScienceDirect

Journal of Aerosol Science

journal homepage: http://www.elsevier.com/locate/jaerosci

Effects of aerosol type and simulated aging on performance of low-cost PM sensors

Jessica Tryner [a,b], John Mehaffy [a], Daniel Miller-Lionberg [b], John Volckens [a,*]

[a] Department of Mechanical Engineering, Colorado State University, 1374 Campus Delivery, Fort Collins, CO, 80523, United States
[b] Access Sensor Technologies, 2401 Research Blvd, Suite 107, Fort Collins, CO, 80526, United States

ARTICLE INFO

Keywords:
Plantower
PMS5003
SPS30
Aerosol light scattering
Photometer
Nephelometer
Optical particle counter

ABSTRACT

Studies that characterize the performance of low-cost particulate matter (PM) sensors are needed to help practitioners understand the accuracy and precision of the mass and number concentrations reported by different models. We evaluated Plantower PMS5003, Sensirion SPS30, and Amphenol SM-UART-04L PM sensors in the laboratory by exposing them to: (1) four different polydisperse aerosols (ammonium sulfate, Arizona road dust, NIST Urban PM, and wood smoke) at concentrations ranging from 10 to 1000 μg m^{-3}, (2) hygroscopic and hydrophobic aerosols (ammonium sulfate and oil) in an environment with varying relative humidity (15%–90%), (3) polystyrene latex spheres (PSL) ranging from 0.1 to 2.0 μm in diameter, and (4) extremely high concentrations of Arizona road dust (18-h mean total PM = 33,000 μg m^{-3}; 18-h mean $PM_{2.5}$ = 7300 μg m^{-3}). Linear models relating PMS5003- and SPS30-reported $PM_{2.5}$ concentrations to TEOM-reported ammonium sulfate concentrations up to 1025 μg m^{-3}, nebulized Arizona road dust concentrations up to 540 μg m^{-3}, and NIST Urban PM concentrations up to 330 μg m^{-3} had $R^2 \geq 0.97$; however, an F-test identified a significant lack of fit between the model and the data for each sensor/aerosol combination. Ratios of filter-derived to PMS5003-reported $PM_{2.5}$ concentrations were 1.4, 1.7, 1.0, 0.4, and 4.3 for ammonium sulfate, nebulized Arizona road dust, NIST Urban PM, wood smoke, and oil mist, respectively. For SPS30 sensors, these ratios were 1.6, 2.1, 2.1, 0.6, and 2.2, respectively. Collocated PMS5003 sensors were less precise than collocated SPS30 sensors when measuring ammonium sulfate, nebulized Arizona road dust, NIST Urban PM, oil mist, or PSL. Our results indicated that particle count data reported by the PMS5003 were not reliable. The number size distribution reported by the PMS5003 (a) did not agree with APS data and (b) remained roughly constant whether the sensors were exposed to 0.1 μm PSL, 0.27 μm PSL, 0.72 μm PSL, 2.0 μm PSL, or any of the other laboratory-generated aerosols. The size distribution reported by the SPS30 did not always agree with APS data, but did shift towards larger particle sizes when the sensors were exposed to 0.72 PSL, 2.0 μm PSL, oil mist, or Arizona road dust from a fluidized bed generator. The proportions of PM mass assigned as PM_1, $PM_{2.5}$, and PM_{10} by all three sensor models shifted as the PSL size increased. After the sensors were exposed to high concentrations of Arizona road dust for 18 h, $PM_{2.5}$ concentrations reported by SPS30 sensors remained consistent, whereas 3/8 PMS5003 sensors and 2/7 SM-UART-04L sensors began reporting erroneously high values.

* Corresponding author.
E-mail addresses: jessica.tryner@colostate.edu (J. Tryner), john.mehaffy@colostate.edu (J. Mehaffy), danlionberg@accsensors.com (D. Miller-Lionberg), john.volckens@colostate.edu (J. Volckens).

https://doi.org/10.1016/j.jaerosci.2020.105654
Received 1 June 2020; Received in revised form 23 August 2020; Accepted 25 August 2020
Available online 2 September 2020

1. Introduction

Human exposure to particulate air pollution is associated with respiratory and cardiovascular morbidity and mortality (Anderson, Thundiyil, & Stolbach, 2012). As a result, exposure to particulate air pollution is consistently identified as a leading risk factor for premature death in studies of the global burden of disease (IHME, 2018). Humans are exposed to particulate matter (PM) outdoors, at home, and at work (Brauer et al., 2016; Farmer et al., 2019; Pillarisetti et al., 2019; Toren, Bergdahl, Nilsson, & Jarvholm, 2007).

Low-cost sensors can help reduce human exposure to PM by identifying the location and timing of elevated PM concentrations. These sensors typically cost $\leq$ $50 each and are often integrated into monitors that cost $\leq$ $300 (Sousan, Koehler, Hallett, & Peters, 2017). Monitors in this price range are accessible to a wide range of practitioners, and low-cost sensors thus have the potential to democratize air quality monitoring (Austen, 2015).

Low-cost sensors typically measure the amount of light scattered by PM to provide real-time data at reduced cost. Although low-cost PM monitors are affordable and tend to be easy to operate, interpretation of the data they provide is not always straightforward. For example, sensor response can vary with changes in particle size and refractive index (even if mass or number concentration remain constant); such changes in aerosol properties can stem from changes in particle sources as well as changes in environmental conditions such as relative humidity (Hagan & Kroll, 2020; Jayaratne, Liu, Thai, Dunbabin, & Morawska, 2018; Levy Zamora et al., 2019; Wang et al., 2015).

Studies that characterize the performance of low-cost PM sensors and evaluate methods for correcting sensor data can help practitioners better understand how these data can be interpreted and utilized. Some sensors report mass concentrations of multiple PM size fractions (e.g., PM_1, $PM_{2.5}$, and PM_{10}) along with number concentrations of particles in a range of size bins between 0.3 and 10 μm. Users of low-cost sensor data may ask: How reliable are these metrics? What are the benefits and limitations of different sensor models? Will sensor performance degrade over time?

In this study, we conducted laboratory experiments to evaluate the performance of three low-cost PM sensors: the PMS5003 (Plantower, Beijing, China), the SPS30 (Sensirion, Stäfa, Switzerland), and the SM-UART-04L (Amphenol Advanced Sensors, St. Marys, PA, USA). The PMS5003 sensor is used in the PurpleAir monitor (www.purpleair.com) and has been studied extensively (Bulot et al., 2019; Delp & Singer, 2020; He, Kuerbanjiang, & Dhaniyala, 2020; Kelly et al., 2017; Magi, Cupini, Francis, Green, & Hauser, 2019; Malings et al., 2020; Sayahi, Butterfield, & Kelly, 2019; Singer & Delp, 2018; Tryner et al., 2020). Few studies have published data from the SPS30 (Kuula et al., 2020). We exposed the sensors to: (1) four different polydisperse aerosols (ammonium sulfate, Arizona road dust, NIST Urban PM, and wood smoke) at concentrations ranging from 10 to 1000 μg m^{-3}, (2) hygroscopic and hydrophobic aerosols (ammonium sulfate and oil) in an environment with varying relative humidity (15%–90%), (3) polystyrene latex spheres (PSL) ranging from 0.1 to 2.0 μm in diameter, and (4) extremely high concentrations of Arizona road dust (18-h mean total PM = 33,000 μg m^{-3}; 18-h mean $PM_{2.5}$ = 7300 μg m^{-3}). These four experiments were designed to answer the following questions: (1) do the sensors respond linearly to $PM_{2.5}$ concentrations ranging up to 1000 μg m^{-3}, (2) how does the relationship between the filter-derived $PM_{2.5}$ concentration and the time-averaged sensor-reported $PM_{2.5}$ concentration vary with aerosol type, (3) how does precision vary between the different sensor models, (4) how are sensor readings affected by high relative humidity, (5) do particle count data reported by the sensors agree with particle count data reported by an Aerodynamic Particle Sizer (APS), (6) do the sensors' assignments of PM to various size fractions (e.g., PM_1, $PM_{2.5}$, PM_{10}) agree with APS data, and (7) do the sensor responses drift over time in a high-concentration environment?

2. Material and methods

2.1. Instrumentation

All of the low-cost PM sensors that we evaluated actively sample air using a small fan, measure the amount of light scattered by particles in the air, and can reportedly detect particles as small as 0.3 μm (Amphenol Advanced Sensors, 2019; Sensirion, 2020; Yong, 2016). In all three sensors, a light detector is oriented perpendicularly to a source of red light ($\lambda \cong$ 650 nm for the PMS5003 and λ = 660 nm for the SPS30 (Kelly et al., 2017; Sensirion, 2020)). Using a polarizer, we determined that the light sourced inside each sensor is polarized perpendicular to the scattering plane.

The Plantower PMS5003 reports mass concentrations of PM_1, $PM_{2.5}$, and PM_{10}. The mass concentration of each size fraction is reported two ways: with a correction factor of one ("CF=1") and with a proprietary correction factor for atmospheric monitoring ("ATM"). The PMS5003 also reports number concentrations (# per 0.1 L) of particles larger than 0.3, 0.5, 1.0, 2.5, 5.0, and 10 μm. The sensor is designed to measure $PM_{2.5}$ concentrations up to 500 μg m^{-3} (Yong, 2016) and retails for approximately $10 to $15 USD, depending on the vendor and quantity purchased.

The Sensirion SPS30 reports mass concentrations of PM_1, $PM_{2.5}$, PM_4, and PM_{10}. The SPS30 also reports the number concentration (# per cm^3) of particles in the following size ranges: 0.3 to 0.5, 0.3 to 1.0, 0.3 to 2.5, 0.3 to 4.0, and 0.3–10 μm. The manufacturer reports that the sensor is calibrated using an atomized potassium chloride aerosol and can measure mass concentrations up to 1000 μg m^{-3} (Sensirion, 2020). The SPS30 has been designed to prevent the sensor elements from becoming contaminated from particle deposition over time. Filtered sheath air flows over the light detector continuously during operation (Lattanzio, 2020). The SPS30 is also pre-programmed to undergo a self-cleaning procedure after every week of continuous operation. During self-cleaning, the fan is accelerated to its maximum speed for 10 s in an effort to remove particles that have accumulated inside the sensor (Sensirion, 2020). Each sensor retails for approximately $30 to $50 USD, depending on the vendor and quantity purchased.

The Amphenol Advanced Sensors SM-UART-04L reports mass concentrations of PM_1, $PM_{2.5}$, and PM_{10}. The mass concentration of each size fraction is reported using two correction factors: "standard smoke" and "environment". The sensor is calibrated using cigarette smoke and can measure mass concentrations up to 999 μg m^{-3} (Amphenol Advanced Sensors, 2019). Each sensor retails for approximately $20 to $30 USD, depending on the vendor and quantity purchased.

Eight PMS5003, eight SPS30, and seven SM-UART-04L sensors were tested. The 23 low-cost sensors were connected to three NUCLEO-F767ZI development boards (STMicroelectronics, Geneva, Switzerland) and controlled using firmware written in Mbed (Arm Mbed, Cambridge, UK). Data from the sensors were visualized and logged every 3 s using a MegunoLink interface (Number Eight Innovation Limited, Hamilton, New Zealand).

All experiments were conducted in a laboratory aerosol chamber with overall dimensions of 1.2 m × 0.85 m × 0.75 m. A continuous flow of compressed, HEPA-filtered dilution air entered the chamber through dozens of holes in pipes that lined the chamber edges. Air was exhausted from the chamber by reference instruments and by a vacuum pump connected to a centrally-located ring duct (with a hole pattern similar to that in the dilution air inlet system). A small fan mixed the air inside the chamber to help maintain a uniform particle concentration throughout. See Supporting Information (SI) Section S1.1 for additional details on the chamber design.

During the experiments, several instruments were used to measure time-averaged PM concentrations, real-time PM concentrations, particle number size distributions, temperature, and relative humidity (RH) in the laboratory chamber. Time-averaged PM concentrations were measured using gravimetric samples collected on 46.2 mm PTFE filters (Tryner et al., 2020). Real-time $PM_{2.5}$ concentrations were measured using a tapered element oscillating microbalance (1405 TEOM, ThermoFisher Scientific, Waltham, MA, USA) that sampled air at 4.0 L min^{-1} with a GK2.05 (KTL) cyclone (Mesa Laboratories, Butler, NJ, USA) on the inlet. The TEOM inlet was heated to 35 °C. Real-time variations in the total PM and/or $PM_{2.5}$ concentration(s) in the chamber were recorded using a DustTrak DRX Aerosol Monitor 8533 (TSI Incorporated, Shoreview, MN, USA). Number size distributions of particles with electrical mobility diameters between 0.0136 and 0.573 μm were measured using a scanning mobility particle sizer (SMPS) (Model 3082 Electrostatic Classifier and Model 3787 Condensation Particle Counter, TSI, Shoreview, MN, USA). Particles passed through a charge neutralizer before entering the SMPS. Number size distributions of particles with aerodynamic diameters between ~0.3 and 19.8 μm were measured using an Aerodynamic Particle Sizer (APS) Spectrometer (3321, TSI Incorporated, Shoreview, MN, USA). Temperature and RH were recorded using an EasyLog WiFi Temperature and Humidity Data Logger (EL-WiFi-TH, Lascar Electronics, Erie, PA, USA).

2.2. Experimental methods

2.2.1. Experiment 1: sensor response to varying aerosol composition and concentration

The sensors' responses to ammonium sulfate, Arizona road dust (Fine Air Cleaner Test Dust, Part No. 1543094, AC Spark Plug Division, General Motors Corporation, Flint, MI, USA), and NIST Urban PM (SRM 1648a, National Institute of Standards and Technology, Gaithersburg, MD, USA) were characterized as described previously (Tryner, Quinn, Windom, & Volckens, 2019; Tryner et al., 2020). Briefly, each aerosol type was nebulized from deionized water using a six-jet Collison nebulizer (CH Technologies, Westwood, NJ, USA). Steady-state $PM_{2.5}$ concentrations of approximately 10, 20, 30, 50, 100, and 250 μg m^{-3} were generated by adjusting (a) the pressure of the compressed air line connected to the nebulizer, (b) the timing of the automated solenoid valve that controlled airflow to the nebulizer, and (c) the flow rate of dilution air into the chamber (Fig. S2). Each concentration was maintained for approximately 45 min. If achievable, steady-state $PM_{2.5}$ concentrations of approximately 500 and 1000 μg m^{-3} were also generated; otherwise, the highest concentration achievable (540 μg m^{-3} for Arizona road dust and 330 μg m^{-3} for NIST Urban PM) was generated and maintained for approximately 45 min.

To characterize the sensors' responses to wood smoke, small pieces of Birch wood (which had been milled to a smooth finish with no bark) were periodically burned and then extinguished in a sealed barrel outside the laboratory aerosol chamber. The compressed air line and solenoid valve (typically used with the nebulizer) were used to direct particulate matter from the barrel into the chamber (Fig. S3). Steady-state $PM_{2.5}$ concentrations of approximately 10, 20, 30, 50, 100, 150, 250, and 500 μg m^{-3} were maintained for approximately 30 min each. These eight steady-state concentrations were generated using smoke from three different combustion events (Fig. S8).

2.2.2. Experiment 2: effect of relative humidity on sensor response

Two tests were conducted to characterize the effect of RH on the sensors' responses. During the first test, an ammonium sulfate concentration of approximately 50 μg m^{-3} was maintained inside the laboratory chamber while RH was varied from 20% to 90%. During the second test, an oil mist concentration of approximately 65 μg m^{-3} was maintained inside the chamber while RH was varied from 15% to 90%.

Both the ammonium sulfate and oil mist aerosols were generated using a Collison nebulizer. Ammonium sulfate was dissolved in deionized water at a concentration of 4.6 g L^{-1}. The oil (Compressor Oil, Item no. 18225, Ace Hardware, Oak Brook, IL, USA; density = 0.867 g cm^{-3}; viscosity = 0.231 Pa s) was placed directly in the nebulizer.

The RH in the aerosol chamber was between 15% and 20% under normal operating conditions (i.e., when dilution air was supplied by HEPA-filtered compressed air). To increase the RH in the chamber, some or all of the dilution air was bubbled through a flask of deionized water that sat on a hot plate (Fig. S4). The fraction of dilution air bubbled through the flask and the temperature of the hot plate were varied to achieve target RH levels of approximately 50%, 60%, 70%, 75%, 80%, and 90%. Each steady-state RH level was maintained for approximately 45 min.

We also included a negative control, in which the chamber RH was maintained at 90% but no aerosols were generated using the nebulizer. All sensors reported time-averaged $PM_{2.5}$ concentrations below 3 μg m^{-3} under these conditions.

2.2.3. Experiment 3: sensor response to aerosols of varying size

We exposed the low-cost sensors to polystyrene latex (PSL) spheres with diameters of 0.10, 0.27, 0.72, and 2.0 μm. For each size, the PSL were suspended in deionized water and aerosolized using the Collison nebulizer. Once the concentration of PSL in the chamber reached steady state, the low-cost sensors, APS, and SMPS measured the particle number size distribution for approximately 15 min (Fig. S5). We also collected data for a negative control in which these instruments measured the "background" particle number size distribution when the nebulizer was operated with deionized water containing no PSL. All sensors reported time-averaged $PM_{2.5}$ concentrations $\leq$1 μg m^{-3} and total counts of 0.3–10 μm particles <3 cm^{-3} under these conditions.

2.2.4. Experiment 4: simulating extended use in a high-concentration environment

To assess the potential for sensor degradation as a result of particle accumulation over time, we exposed the sensors to extremely high concentrations of Arizona road dust aerosol for a total of 18 h. Arizona road dust aerosol was generated using a fluidized bed aerosol generator (3400A, TSI Incorporated, Shoreview, MN, USA) (Fig. S6). The sensors were exposed to Arizona road dust aerosol in six 3-h long segments. Before and after each segment, the sensors were separately exposed to nebulized NIST Urban PM concentrations of 0, 10, 30, and 50 μg m^{-3} and their responses were evaluated (Fig. S7).

During the six Arizona road dust exposure periods, the $PM_{2.5}$ and total PM concentrations inside the laboratory chamber were monitored using the DustTrak (with no size-selective inlet). Filter samples were collected to determine the gravimetric correction factors for the real-time $PM_{2.5}$ and total PM concentrations reported by the DustTrak. Four of these were $PM_{2.5}$ filter samples collected with 46.2-mm diameter PTFE filters installed downstream of 16.7 L min^{-1} 2.5 μm cyclones. One was a total PM sample collected with a 46.2-mm diameter PTFE filter installed in an open-faced filter cassette. Each filter sample lasted approximately 20 min.

The DustTrak reported mean filter-corrected $PM_{2.5}$ and total PM concentrations of 7300 and 33,000 μg m^{-3}, respectively, during the 18-hr Arizona road dust exposure period. These concentrations would be equivalent to exposing the low-cost sensors to continuous $PM_{2.5}$ and total PM concentrations of 15 μg m^{-3} and 70 μg m^{-3}, respectively, for 360 days (~1 year).

The Sensirion SPS30 is pre-programmed to undergo a self-cleaning procedure once per week (i.e., every 604,800 s). Because this experiment was designed to simulate 360 days in 18 h, the self-cleaning interval for the SPS30 sensors was adjusted to 1260 s during the exposures to Arizona road dust. Self-cleaning was turned off during the evaluation periods.

2.3. Data analyses

Several corrections were made to the SMPS and APS data before performing the analyses described below. These corrections are described in SI Section S1.3. First, APS data were corrected by dividing the number concentration reported at each aerodynamic diameter by a size-specific liquid (for oil mist particles) or solid (for all other aerosols) particle counting efficiency (Volckens & Peters, 2005). Second, electrical mobility diameters reported by the SMPS (d_m) and aerodynamic diameters reported by the APS (d_a) were converted to volume equivalent diameters (d_{ve}) (DeCarlo, Slowik, Worsnop, Davidovits, & Jimenez, 2004).

2.3.1. Sensor response to varying aerosol composition and concentration

We used data from Experiment 1—in which the low-cost sensors were exposed to varying concentrations of ammonium sulfate, Arizona road dust, NIST Urban PM, and wood smoke—to investigate whether the sensors responded linearly to $PM_{2.5}$ concentrations ranging up to 1000 μg m^{-3}. For the ammonium sulfate, Arizona road dust, and NIST Urban PM aerosols, the time-averaged $PM_{2.5}$ concentration reported by each low-cost sensor model ($\bar{c}_{sensor}$; μg m^{-3}) was compared to the time-averaged $PM_{2.5}$ concentration reported by the TEOM ($\bar{c}_{TEOM}$; μg m^{-3}) as shown in Equation (1):

$$\bar{c}_{sensor} = \beta_0 + \beta_1 \bar{c}_{TEOM} + \varepsilon \quad (1)$$

where β_0 was the y-intercept, β_1 was the slope, and ε was the random error. In Equation (1), the time-averaging period was the duration of steady-state concentration point *i*. The linear model shown in Equation (1) was fit using weighted least-squares regression and an F-test was conducted to determine whether there was a significant lack of fit between the data and the model (Analytical Methods Committee, 1994).

We also used data from Experiment 1 and the Experiment 2 test with oil mist to investigate how the relationship between the filter-derived $PM_{2.5}$ concentration and the sensor-reported $PM_{2.5}$ concentration varied with aerosol type. For each aerosol, we compared the mean time-averaged $PM_{2.5}$ concentration derived from the three concurrent, collocated filter samples (c_{filter}; μg m^{-3}) to the time-averaged $PM_{2.5}$ concentration reported by each low-cost sensor *j* ($\bar{c}_{sensor,j}$; μg m^{-3}) as shown in Equation (2):

$$CF_j = c_{filter} / \bar{c}_{sensor,j} \quad (2)$$

where CF_j represents a gravimetric correction factor for low-cost sensor *j*. In Equation (2), the time-averaging period was the duration of the entire test with a given aerosol. Multiplying a sensor's output by CF_j would establish equivalence between the time-averaged concentrations reported by the sensor and derived from the filter samples.

Next, we investigated whether differences in the gravimetric correction factors (*CF* in Equation (2)) and linear model slopes (β_1 in Equation (1)) calculated for different sensor/aerosol combinations were consistent with Mie theory. We used the Python package PyMieScatt to predict scattering intensity as a function of scattering angle for the aerosols measured during each nonzero steady-state concentration point in Experiment 1 and each RH level in the Experiment 2 test with oil mist (Sumlin, Heinson, & Chakrabarty, 2018).

The "SF_SD" function from PyMieScatt takes the particle refractive index, incident light wavelength, a vector of particle diameters, and a corresponding vector of particle counts as inputs (Sumlin, 2020). The refractive index assumed for each aerosol is listed in Table S1. The incident light wavelength was assumed to be 660 nm (Sensirion, 2020). Particle number size distributions were derived from SMPS and APS data for particles $\leq$ 2.5 μm. We multiplied particle number concentrations from the SMPS and APS data by the volume illuminated when the light source passed over the detector in the PMS5003. We divided the scattering intensity calculated using PyMieScatt by the time-averaged TEOM-reported $PM_{2.5}$ concentration ($\bar{c}_{TEOM}$; μg m^{-3}) for the relevant concentration point to obtain the scattering intensity per 1 μg m^{-3}.

2.3.2. Sensor precision

We used data from Experiments 1, 2, and 3 to assess how precision varied between sensor models. First, we used the relative standard deviation to quantify the precision of the $PM_{2.5}$ concentrations measured by all J sensors of a given model at each nonzero steady-state concentration point i in Experiment 1, at each steady-state RH level i in Experiment 2, and for each PSL size in Experiment 3:

$$RSD_i = \frac{s_i}{(1/J)\sum \bar{c}_{ij}} \tag{6}$$

where s_i was the sample standard deviation of the time-averaged $PM_{2.5}$ concentrations reported by all J sensors during point i and $\bar{c}_{ij}$ was the time-averaged $PM_{2.5}$ concentration reported by sensor j during point i. We also quantified precision using Equation S4 to facilitate comparisons to a wider range of prior studies (Camalier, Eberly, Miller, & Papp, 2007; Malings et al., 2020).

2.3.3. Effect of relative humidity on sensor response

The effect that changes in RH had on sensor-reported $PM_{2.5}$ mass concentrations was assessed using data from the Experiment 2, which consisted of one test with a hygroscopic aerosol (ammonium sulfate) and one test with a hydrophobic aerosol (oil mist). During each test, the $PM_{2.5}$ concentration was maintained at ~50 μg m^{-3} while RH was intentionally varied from $\leq$20% up to 90%. During the test with ammonium sulfate, the dry $PM_{2.5}$ concentration in the chamber ($c_{TEOM,\ dry}$; μg m^{-3}) was calculated by correcting the TEOM-reported concentration (c_{TEOM}; μg m^{-3}) using κ-Köhler theory:

$$c_{dry} = \frac{c_{wet}}{1 + \kappa \frac{\rho_w}{\rho_s}\left(\frac{a_w}{1-a_w}\right)} \tag{7}$$

where κ was the hygroscopicity parameter for ammonium sulfate (0.53), ρ_w was the density of liquid water (1000 kg m^{-3}), ρ_s was the density of solid ammonium sulfate (1770 kg m^{-3}), and a_w was the water activity (assumed to be equal to RH expressed as a number between 0 and 1) (Kreidenweis & Asa-Awuku, 2014; Petters & Kreidenweis, 2007). The RH in the 35 °C TEOM inlet was calculated by assuming that the absolute humidity was the same in the chamber and the TEOM inlet (Table S2). Although the TEOM inlet was heated to dry the incoming aerosol, the RH in the TEOM inlet remained above the efflorescence RH for ammonium sulfate (35%) when the RH inside the chamber was $\geq$60%. The test-averaged value of $\bar{c}_{TEOM,dry}$ differed from the mean $PM_{2.5}$ concentration derived from the three filter samples (which spanned the test duration) by only 0.34%. This agreement supported the assumption that values of $c_{TEOM,\ dry}$ calculated using Equation (7) accurately reflected the dry $PM_{2.5}$ concentration inside the chamber.

Table 1
Equations used to calculate the total particle counts, total PM mass, fraction of particle counts, and fraction of PM mass assigned to each size bin reported by the low-cost sensors. $PN_{X.X}$ represents the number concentration (# cm^{-3}) of particles between 0.3 and X.X μm. The Plantower PMS5003 reports counts of particles larger than 0.3, 0.5, 1.0, 2.5, 5.0, and 10 μm; the Sensirion SPS30 reports counts of particles between 0.3 and 0.5, 0.3 and 1.0, 0.3 and 2.5, 0.3 and 4.0, as well as 0.3 and 10 μm; and the Amphenol SM-UART-04L reports no particle count data. $PM_{X.X}$ represents the mass concentration (μg m^{-3}) of particles smaller than X.X μm. All three sensors report PM_1, $PM_{2.5}$, and PM_{10} mass concentrations. The Sensirion SPS30 also reports a PM_4 mass concentrations.

Lower limit (μm)	Upper limit (μm)	Total	Fraction
Particle count bins			
0.3	0.5	$PN_{0.5}$	$PN_{0.5}/PN_{10}$
0.5	1.0	$PN_{1.0} - PN_{0.5}$	$(PN_{1.0} - PN_{0.5})/PN_{10}$
1.0	2.5	$PN_{2.5} - PN_{1.0}$	$(PN_{2.5} - PN_{1.0})/PN_{10}$
2.5	4.0 or 5.0	$PN_{4.0/5.0} - PN_{2.5}$	$(PN_{4.0/5.0} - PN_{2.5})/PN_{10}$
4.0 or 5.0	10.0	$PN_{10} - PN_{4.0/5.0}$	$(PN_{10} - PN_{4.0/5.0})/PN_{10}$
Particulate matter mass bins			
0.3	1.0	$PM_{1.0}$	$PM_{1.0}/PM_{10}$
1.0	2.5	$PM_{2.5} - PM_{1.0}$	$(PM_{2.5} - PM_{1.0})/PM_{10}$
2.5	4.0	$PM_{4.0} - PM_{2.5}$	$(PM_{4.0} - PM_{2.5})/PM_{10}$
2.5	10.0	$PM_{10} - PM_{2.5}$	$(PM_{10} - PM_{2.5})/PM_{10}$
4.0	10.0	$PM_{10} - PM_{4.0}$	$(PM_{10} - PM_{4.0})/PM_{10}$

For each steady-state RH level i, we first calculated the ratio of the time-averaged $PM_{2.5}$ concentration reported by each low-cost sensor j to the time-averaged $PM_{2.5}$ concentration reported by the TEOM ($\overline{c}_{sensor,ij}/\overline{c}_{TEOM,dry,i}$ for the test with ammonium sulfate and $\overline{c}_{sensor,ij}/\overline{c}_{TEOM,i}$ for the test with oil mist). Then, we used Equation (7) to estimate the dry ammonium sulfate concentrations measured by the low-cost sensors and calculated $\overline{c}_{sensor,dry,ij}/\overline{c}_{TEOM,dry,i}$. When calculating $\overline{c}_{sensor,dry,ij}$, a_w was assumed to be equal to the RH inside the laboratory chamber.

2.3.4. Comparison of sensor- and APS-Reported particle number concentrations

We compared the number concentrations of 0.3–10 μm particles reported by the low-cost sensors and the APS. The number concentrations (# cm^{-3}) assigned to five size bins by the Plantower PMS5003 and Sensirion SPS30 sensors were calculated as shown in Table 1. Number concentrations derived from APS data in approximately 40 bins with midpoint diameters ≤10 μm were then aggregated into the five size bins reported by each low-cost sensor model. Note that the smallest particles detected by the APS are reported in a single bin with an upper limit of $d_a = 0.523$ μm. The lower limit of this bin was taken to be $d_a \approx 0.3$ μm, and all particles in APS bins with midpoint $d_{ve} < 0.5$ μm were assigned to the 0.3–0.5 μm size bin.

For data recorded while the sensors measured ~50 μg m^{-3} concentrations ammonium sulfate, Arizona road dust, NIST Urban PM, and wood smoke (Experiment 1) and a 61 μg m^{-3} concentration of oil mist at RH = 15% (Experiment 2), the number concentration reported in each size bin by each low-cost sensor was divided by the number concentration in the same size bin as derived from APS data to determine whether the low-cost sensor underreported, correctly-reported, or overreported the concentration of particles in that range.

2.3.5. Comparison of sensor- and APS-Reported particle number and mass distributions

We used data recorded while the sensors measured ~50 μg m^{-3} concentrations of ammonium sulfate, Arizona road dust, NIST Urban PM, and wood smoke (Experiment 1); a 61 μg m^{-3} concentration of oil mist at RH = 15% (Experiment 2); 0.10, 0.27, 0.72, and 2.0 μm PSL (Experiment 3); and Arizona road dust aerosol from the fluidized bed generator (Experiment 4) to compare particle number size distributions reported by the low-cost sensors and the APS. The particle count data reported by the Plantower PMS5003 and Sensirion SPS30 sensors were used to calculate the fraction of particle counts assigned to each size bin as shown in Table 1.

We also used data from Experiment 3 to investigate whether the sensors' assignments of PM mass to various size fractions agreed with APS data. The PM_1, $PM_{2.5}$, $PM_{4.0}$, and PM_{10} concentrations reported by the Plantower PMS5003, Sensirion SPS30, and Amphenol SM-UART-04L sensors were used to calculate the fraction of particle mass assigned to each of the mass bins listed in Table 1.

In addition, particle count data reported by the PMS5003 and SPS30 sensors during Experiment 3 were used to calculate the PM

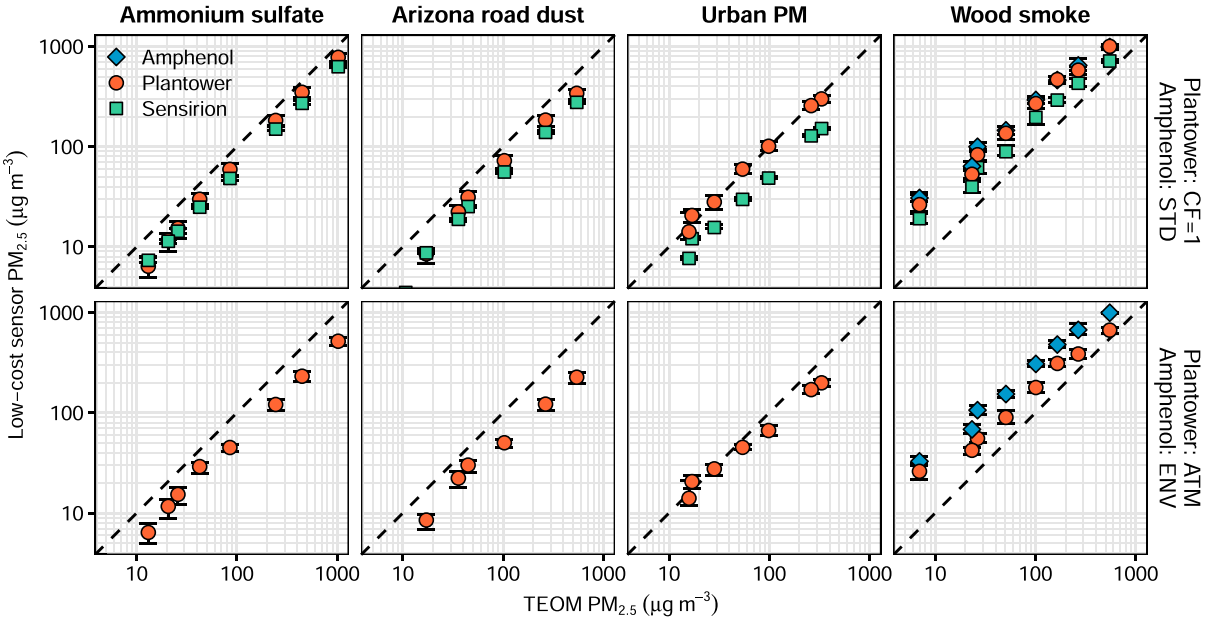

Fig. 1. $PM_{2.5}$ concentrations reported by Plantower PMS5003, Sensirion SPS30, and Amphenol SM-UART-04L sensors compared to $PM_{2.5}$ concentrations reported by the TEOM. The dashed line represents y = x. Markers and error bars represent the mean and total range of $PM_{2.5}$ concentrations reported by all seven or eight sensors. Concentrations reported by PMS5003 and SM-UART-04L sensors using "CF=1" and "standard smoke" correction factors, respectively, are shown in the top row. Concentrations reported by PMS5003 and SM-UART-04L sensors using "atmospheric" and "environment" correction factors, respectively, are shown in the bottom row. Concentrations reported by the SPS30, which does not report data using multiple correction factors, are shown in the top row only. SM-UART-04L data are not shown in the first three columns because those sensors were not tested with ammonium sulfate, Arizona road dust, or NIST Urban PM. Ammonium sulfate, Arizona road dust, and NIST Urban PM were aerosolized using a nebulizer.

concentrations in each mass bin listed in Table 1. For example, the PM_1 concentration was calculated from the number concentrations in the 0.3–0.5 and 0.5–1.0 μm size bins. Each particle was assumed to be spherical with a diameter equal to the geometric mean of the lower and upper bin limits. The mass distributions derived from the count data were compared to the mass distributions derived from the PM_1, $PM_{2.5}$, $PM_{4.0}$, and PM_{10} concentrations reported directly by the sensors.

2.3.6. Sensor response after simulating extended use in a high-concentration environment

We used data from Experiment 4—in which the low-cost sensors were exposed to time-averaged Arizona road dust $PM_{2.5}$ and total PM concentrations of 7300 and 33,000 μg m^{-3} during six 3-h long segments—to investigate whether the sensor responses drifted over time in a high-concentration environment. Before the first and after each Arizona road dust exposure, the sensors' responses to nebulized NIST Urban PM concentrations of 0, 10, 30, and 50 μg m^{-3} were recorded. The precision of the $PM_{2.5}$ concentrations measured at each nonzero steady-state concentration point i by all J sensors of a given model was quantified using the RSD_Q metric, which is an alternative to the relative standard deviation that is more suitable for use with values that are not normally distributed (Arachchige, Prendergast, & Staudte, 2019):

$$RSD_{Q,i} = 0.75\frac{IQR_i}{median\left(\bar{c}_{ij}\right)} \tag{8}$$

where IQR_i was the interquartile range of the time-averaged $PM_{2.5}$ concentrations reported by all J sensors during concentration point i and $\bar{c}_{ij}$ was the time-averaged $PM_{2.5}$ concentration reported by sensor j during concentration point i.

3. Results and discussion

3.1. Sensor response to varying aerosol composition and concentration

The $PM_{2.5}$ concentrations reported by the low-cost sensors and the TEOM during Experiment 1 are compared in Fig. 1, S9, and S10. Plantower PMS5003 "CF=1" values underestimated ammonium sulfate and Arizona road dust concentrations but correctly estimated NIST Urban PM concentrations (compared to the TEOM). The Sensirion SPS30 reported lower $PM_{2.5}$ concentrations than the PMS5003 ("CF=1" values) for all four aerosols (i.e., the SPS30 underestimated ammonium sulfate, Arizona road dust, and NIST Urban PM concentrations relative to the TEOM). All three sensors overestimated TEOM-reported wood smoke $PM_{2.5}$ concentrations. Neither the PMS5003-reported $PM_{2.5}$ "CF=1" values nor the SPS30-reported $PM_{2.5}$ values appeared saturated at any of the concentration points measured in Experiment 1. The SM-UART-04L did not report $PM_{2.5}$ concentrations above 999 μg m^{-3}.

Linear models (Equation (1)) fit to relate the PMS5003 CF=1- and TEOM-reported $PM_{2.5}$ concentrations had coefficients of determination (R^2) $\geq$ 0.97. Similarly, linear models fit to relate the SPS30- and TEOM-reported $PM_{2.5}$ concentrations had $R^2 \geq 0.98$; however, the F test identified a significant lack of fit between the data and each of the six linear models (Table S4). The weighted residuals for these models increased with the TEOM-reported $PM_{2.5}$ concentration, reached a peak, and then decreased as the TEOM-reported concentration increased further (Fig. S11). These patterns suggested that Equation (1) might not have been the best model to specify for these low-cost sensors over the range of $PM_{2.5}$ concentrations tested in Experiment 1. Users who wish to apply Equation (1) to correct $PM_{2.5}$ concentrations output by PMS5003 or SPS30 sensors should consider whether assuming a linear response would

Table 2
Data from the ammonium sulfate, Arizona road dust, NIST Urban PM, and wood smoke tests conducted during Experiment 1 as well as the oil mist test conducted during Experiment 2. Ammonium sulfate, Arizona road dust, NIST Urban PM, and oil were aerosolized using a nebulizer. Particle size statistics: Count median diameters (CMD), mass median diameters (MMD) and geometric standard deviations (GSD) calculated from volume equivalent diameters. For each metric, the median and total range calculated across all steady-state points for which SMPS and APS data were available are shown. Gravimetric correction factors: *CF* from Equation (2) for $PM_{2.5}$ concentrations reported by Plantower PMS5003 ("CF=1" values), Sensirion SPS30, and Amphenol SM-UART-04L ("standard smoke" values) sensors. For each aerosol/sensor combination, the median and total range of the correction factors calculated across all seven or eight sensors are shown. SM-UART-04L sensors were not tested with ammonium sulfate, Arizona road dust, or NIST Urban PM. Scattering intensity: Intensity of perpendicular polarized, parallel polarized, and unpolarized 660 nm light scattered at 90°, per 1 μg m^{-3} of $PM_{2.5}$. For each aerosol/polarization combination, the median and total range of the intensities calculated across all steady-state points for which SMPS and APS data were available are shown.

	Ammonium sulfate	Arizona road dust	NIST Urban PM	Wood smoke	Oil mist
Particle size statistics					
CMD (μm)	0.041 [0.039–0.044]	0.028 [0.025–0.030]	0.036 [0.035–0.037]	0.12 [0.097–0.30]	0.14 [0.040–0.76]
MMD (μm)	1.1 [0.79–1.2]	0.83 [0.45–0.91]	0.64 [0.49–0.74]	0.42 [0.40–0.54]	2.9 [2.8–2.9]
GSD	2.3 [2.2–2.3]	2.1 [2.0–2.3]	2.0 [1.9–2.2]	3.2 [2.2–3.9]	4.1 [3.1–5.6]
Gravimetric correction factors					
Plantower PMS5003	1.4 [1.3, 1.5]	1.7 [1.5, 2.0]	1.0 [1.0, 1.1]	0.4 [0.4, 0.5]	4.3 [3.6, 6.1]
Sensirion SPS30	1.6 [1.6, 1.7]	2.1 [2.0, 2.1]	2.1 [2.0, 2.1]	0.6 [0.6, 0.7]	2.2 [2.0, 2.5]
Amphenol SM-UART-04L	–	–	–	0.3 [0.3, 0.3]	2.6 [1.5, 13.5]
Scattering intensity (× 100)					
Perpendicular polarized	5.5 [5.0, 5.8]	4.0 [1.2, 4.6]	6.2 [5.1, 7.5]	9.9 [8.9, 11.3]	5.0 [4.5, 5.5]
Parallel polarized	6.0 [4.9, 6.4]	3.6 [0.9, 4.8]	3.2 [2.5, 5.0]	8.0 [7.1, 10.5]	9.3 [8.4, 10.3]
Unpolarized	5.8 [5.1, 6.0]	3.8 [1.1, 4.7]	4.5 [4.2, 6.3]	8.8 [8.4, 10.9]	7.1 [6.4, 7.9]

introduce unacceptable bias given their application and the range of $PM_{2.5}$ concentrations they expect to measure.

For wood smoke, $PM_{2.5}$ concentrations reported by the PMS5003 ("CF=1" values), SPS30, and SM-UART-04L ("standard smoke" values) increased in a manner that was clearly nonlinear relative to the TEOM-reported $PM_{2.5}$ concentration (Fig. 1 and S9). These nonlinear increases may have occurred because the aerosols measured during the different concentration points had different particle number size distributions (Fig. S14). The aerosols measured during the eight concentration points were generated during three different combustion events (Fig. S8). In addition, the aerosols used to produce the steady-state concentration points measured after each combustion event had been aged in the combustion chamber for different periods of time. Error in the TEOM measurement might have also contributed to these nonlinear increases. The time-averaged $PM_{2.5}$ concentration measured by the TEOM during the test with wood smoke was 46% higher than the mean $PM_{2.5}$ concentration derived from the filter samples (for comparison, the time-averaged $PM_{2.5}$ concentrations measured by the TEOM were within 6% of the mean filter-derived $PM_{2.5}$ concentrations for the Experiment 1 tests with ammonium sulfate, Arizona road dust, and NIST Urban PM; Table S3).

Count median diameters (CMDs) and mass median diameters (MMDs) for each of the four aerosols shown in Fig. 1 are listed in Table 2. CMDs of 0.025–0.044 μm for ammonium sulfate, Arizona road dust, and NIST Urban PM indicated that most of the particles, by count, were smaller than 0.3 μm. Particles smaller than ~0.3 μm would not have been detected by the low-cost sensors, but would have been measured by the TEOM (which captures particles on a filter and is therefore not subject to the 0.3 μm detection limit); however, MMDs ranging from 0.45 to 1.2 μm for these same aerosols indicated particles larger than 0.3 μm accounted for the majority of aerosol mass (Fig. S13).

The intensity of perpendicular-polarized light that Mie theory predicted would be scattered at 90° (per 1 μg m^{-3} $PM_{2.5}$) was generally consistent with the response of the PMS5003 to ammonium sulfate and Arizona road dust (relative to NIST Urban PM; Table 2). The median intensities of perpendicular-polarized light scattered by ammonium sulfate and nebulized Arizona road dust were 89% and 65%, respectively, of the median intensity of perpendicular-polarized light scattered by NIST Urban PM. These results were consistent with the observation that the PMS5003 correctly-estimated NIST Urban PM concentrations, relative to the TEOM and filter samples, but underestimated ammonium sulfate and Arizona road dust concentrations. The slopes of linear models relating PMS5003- and TEOM-reported $PM_{2.5}$ concentrations were 0.75 and 0.67 for ammonium sulfate and Arizona road dust, respectively, compared to 0.98 for NIST Urban PM (Table S4).

The intensity of perpendicular-polarized light scattered by NIST Urban PM was 62% of the intensity of perpendicular-polarized light scattered by wood smoke (Table 2). This result was consistent with the observation that the PMS5003 overestimated wood smoke concentrations. The high wood smoke $PM_{2.5}$ concentrations reported by the low-cost sensors were attributed to the higher CMD of the wood smoke (0.097–0.30 μm) compared to ammonium sulfate, Arizona road dust, and NIST Urban PM. In other words, the wood smoke consisted of more particles, by number, above the sensors' ~0.3 μm optical detection limit (Fig. S12). The gravimetric correction factor of 0.4 needed to bring the test-averaged $PM_{2.5}$ "CF=1" concentration reported by the PMS5003 into agreement with the mean test-averaged $PM_{2.5}$ concentration derived from collocated filter samples agreed with results from another recent study in which low-cost outdoor monitors using the PMS5003 overestimated concentrations of $PM_{2.5}$ from wildfire smoke in California and Utah, USA by a factor of two (Delp & Singer, 2020).

The intensity of perpendicular-polarized light that Mie theory predicted the oil mist would scatter at 90° (per 1 μg m^{-3} $PM_{2.5}$) was *not* consistent with the response of the PMS5003 (relative to NIST Urban PM). The PMS5003 sensor severely underestimated oil mist concentrations. Oil mist had the largest CMD and MMD of the five aerosols listed in Table 2, but larger particles might have been preferentially lost in the tortuous flow path between the PMS5003 inlet and the particle sensing zone (Sayahi et al., 2019).

The relative response of the SPS30 to each of the four aerosols tested in Experiment 1 was most consistent with the intensity of parallel-polarized light that Mie theory predicted would be scattered at 90° (per 1 μg m^{-3} $PM_{2.5}$) (Table 2). Both the SPS30 and the PMS5003 appeared to source perpendicular polarized light from a ~660 nm laser and detect scattered light using a photodiode, so this inconsistency might indicate that the SPS30 uses a fundamentally different algorithm to predict PM concentrations (Lattanzio, 2020). Like the PMS5003, the SPS30 overestimated wood smoke $PM_{2.5}$ concentrations and underestimated oil mist $PM_{2.5}$ concentrations.

Although the SPS30 reported lower $PM_{2.5}$ concentrations than the PMS5003 for all four aerosols tested during Experiment 1, the SPS30 reported higher $PM_{2.5}$ concentrations than the PMS5003 when measuring oil mist (Experiment 2) and when measuring Arizona road dust aerosolized using the fluidized bed generator (Experiment 4; Fig. S16). These results might have indicated that (a) large particle losses were more severe in the PMS5003 and (b) the PMS5003 became saturated at a lower $PM_{2.5}$ concentration than the SPS30. When measuring Arizona road dust aerosolized using the fluidized bed generator, the ratio of the filter-corrected DustTrak-reported $PM_{2.5}$ concentration to the SPS30-reported $PM_{2.5}$ concentration was approximately 1.7.

Despite the agreement between NIST Urban PM concentrations reported by the PMS5003 and derived from the filter samples, studies in various U.S. cities have revealed that PMS5003 sensors tend to overestimate ambient $PM_{2.5}$ concentrations when compared to reference monitors (Magi, Cupini, Francis, Green, & Hauser, 2019; Malings et al., 2020; Tryner et al., 2020). Although some of this overestimation was attributed to hygroscopic growth of aerosols at high ambient RH, PMS5003 sensors still tended to overestimate reference $PM_{2.5}$ concentrations when RH remained low. Together, these results suggest that nebulized NIST Urban PM—which is prepared from urban particulate matter collected near St. Louis, MO in 1976 and 1977—differs from present-day ambient aerosol mixtures in the U.S. (Gonzalez & Watters, Jr., 2015).

The analyses presented above are subject to several limitations. First, we assumed that TEOM-reported $PM_{2.5}$ concentrations were accurate and increased linearly with the true $PM_{2.5}$ concentration. Test-averaged $PM_{2.5}$ concentrations reported by the TEOM and derived from the filter samples are compared in Table S3. Second, we assumed that aerosols measured by the low-cost sensors during Experiment 1 were dry, even though these aerosols did not pass through a drier after exiting the nebulizer or the combustion chamber. The aerosol chamber RH was typically <25%; however, if the ammonium sulfate, Arizona road dust, NIST Urban PM, or wood smoke

particles measured by the low-cost sensors contained water that evaporated in the heated TEOM inlet and from the conditioned filter samples, gravimetric correction factors listed in Table 2 would be underestimated and linear model slopes listed in Table S4 would be overestimated. Third, errors in the particle number size distributions derived from SMPS and APS data as well as uncertainties in the densities, shape factors, and refractive indices assumed for each aerosol might have contributed to discrepancies between the measured gravimetric correction factors and the relative scattering intensities predicted using Mie theory.

3.2. Sensor precision

The relative standard deviation (RSD) of the $PM_{2.5}$ concentrations reported by the seven or eight sensors of each type is shown in Fig. 2 for each nonzero concentration point from Experiment 1, each RH level from Experiment 2, and each PSL size from Experiment 3. The Sensirion SPS30 had a lower RSD than the Plantower PMS5003 when exposed to ammonium sulfate, Arizona road dust, NIST Urban PM, oil mist, and PSL. This lower RSD indicated better agreement between the $PM_{2.5}$ concentrations reported by all eight sensors.

All three sensor models had similar RSDs when exposed to wood smoke. During the wood smoke test, PMS5003 RSDs were similar to those observed during the other three Experiment 1 tests; however, SPS30 RSDs were higher than observed during the other three Experiment 1 tests. The reason for the higher SPS30 RSDs is unknown, but the wood smoke had a larger CMD and contained more semi-volatile particles than the other aerosols tested in Experiment 1 (Table 2).

RSD values calculated for the SM-UART-04L were similar to those calculated for the PMS5003 at most RH levels measured during the Experiment 2 test with ammonium sulfate. RSDs >30%, which were calculated for the SM-UART-04L during the test with oil mist (and at two RH levels in the test with ammonium sulfate), resulted from one of the seven sensors reporting abnormally low $PM_{2.5}$ concentrations.

The increasing RSDs observed with increasing PSL size suggested that particle size affected the precision of the low-cost sensors; however, interpretation of these results was complicated by variations in the total $PM_{2.5}$ concentration between the tests with different PSL sizes. The sensors reported lower $PM_{2.5}$ concentrations when measuring 2.0 μm PSL (PMS5003: 2–4 μg m^{-3}; SPS30: 9–12 μg m^{-3}; SM-UART-04L: 9–22 μg m^{-3}) than when measuring smaller PSL (PMS5003: 31–137 μg m^{-3}; SPS30: 28–83 μg m^{-3}; SM-UART-04L: 50–126 μg m^{-3}). RSD values calculated for PMS5003 and SPS30 sensors measuring oil mist (17%–27% and 7%–8%, respectively)

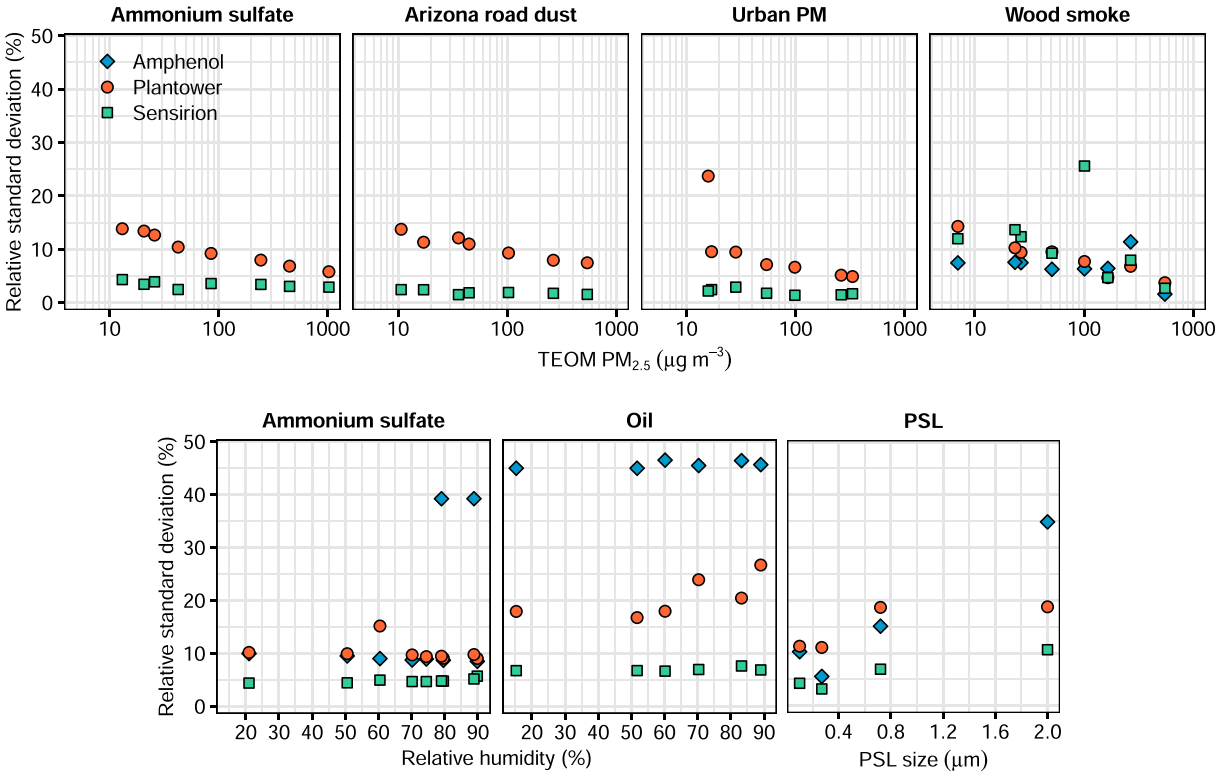

Fig. 2. Relative standard deviations of $PM_{2.5}$ concentrations reported by the Plantower PMS5003 ("CF=1" values), Sensirion SPS30, and Amphenol SM-UART-04L ("standard smoke" values) sensors at each nonzero concentration point from in Experiment 1 (top row), at each RH level from Experiment 2 (bottom left), and for each PSL size from Experiment 3 (bottom right). SM-UART-04L sensors were not included in the Experiment 1 tests with ammonium sulfate, Arizona road dust, or NIST Urban PM. Relative standard deviations above 30% were observed during some RH levels from Experiment 2 because a single SM-UART-04L sensor reported abnormally low concentrations.

also supported the hypothesis that higher RSDs were related to larger particles. The homogeneity of the PM concentration throughout the aerosol chamber could have decreased as particle size increased; however, $PM_{2.5}$ concentrations derived from two filter samples collected ~0.75 m apart during the test with oil mist differed by < 5% (Table S3).

Overall, RSDs calculated for PMS5003 sensors were typically <15% (except for when the sensors measured oil mist, 0.72 μm PSL, or 2.0 μm PSL). RSDs calculated for SPS30 sensors were typically <10% (except for when the sensors measured wood smoke or 2.0 μm PSL). These RSDs were lower than the ~25% RSD reported for 14 Alphasense OPC-N2 sensors measuring ambient aerosols (Crilley et al., 2018). In addition, precision values calculated using Equation S4 (Fig. S17) were almost always lower than the median precision of ~60% reported for uncorrected ambient $PM_{2.5}$ concentrations measured using PurpleAir monitors (Malings et al., 2020). These comparisons suggest that low-cost sensors might produce less precise measurements when operating in the field than when operating in a laboratory.

3.3. Effect of relative humidity on sensor response

During the test with ammonium sulfate, the ratio of the time-averaged sensor-reported $PM_{2.5}$ concentration to the dry, time-averaged TEOM-reported $PM_{2.5}$ concentration ($\bar{c}_{sensor}/\bar{c}_{TEOM,dry}$) increased as the RH inside the chamber increased from 21% to 90% (Fig. 3). For 50% ≤ RH ≤ 70%, the mean value of $\bar{c}_{sensor}/\bar{c}_{TEOM,dry}$ (averaged over all J sensors of a given model) remained within 40% of the value calculated at RH = 21%. The $\bar{c}_{sensor}/\bar{c}_{TEOM,dry}$ ratio then increased sharply for RH ≥ 74% (Fig. S19). These results were expected given that ammonium sulfate is hygroscopic with a deliquescence RH of 80% (Kreidenweis & Asa-Awuku, 2014).

During the Experiment 2 test with oil mist, the ratio of the time-averaged sensor- and TEOM-reported $PM_{2.5}$ concentrations did not increase as RH increased from 15% to 89% (Fig. 3 and Figs. S18–S19). This result was expected given that the oil mist is hydrophobic and therefore does not absorb water as RH increases.

When dry ammonium sulfate $PM_{2.5}$ concentrations were estimated from the low-cost sensor measurements using Equation (7), the $\bar{c}_{sensor,\ dry}/\bar{c}_{TEOM,dry}$ ratio decreased as the RH in the chamber increased beyond 60% (Fig. 3). For the PMS5003 and SM-UART-04L sensors, The mean $\bar{c}_{sensor,\ dry}/\bar{c}_{TEOM,dry}$ ratio remained within 15% of the value calculated at RH = 21% for RH values up to 80%;

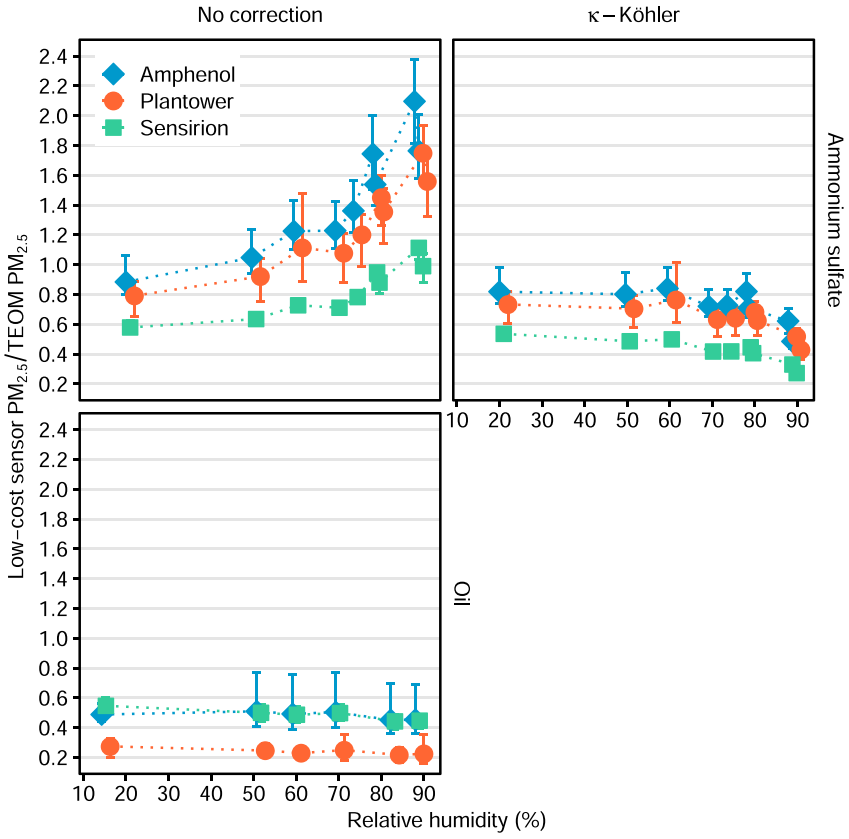

Fig. 3. Left: Variation in the ratio of the time-averaged sensor-reported $PM_{2.5}$ concentration to the time-averaged TEOM-reported $PM_{2.5}$ concentration with increasing relative humidity ($\bar{c}_{sensor}/\bar{c}_{TEOM,dry}$ for the test with ammonium sulfate and $\bar{c}_{sensor}/\bar{c}_{TEOM}$ for the test with oil). Top: Comparison of $\bar{c}_{sensor}/\bar{c}_{TEOM,dry}$ and $\bar{c}_{sensor,\ dry}/\bar{c}_{TEOM,dry}$ ratios for the test with ammonium sulfate aerosol. Markers and error bars represent the mean and total range of the ratios calculated for all seven or eight sensors. All ratios were calculated using PMS5003 $PM_{2.5}$ "CF=1" values, SPS30 $PM_{2.5}$ values, and SM-UART-04L $PM_{2.5}$ "standard smoke" values.

however at RH = 90%, the mean $\overline{c}_{sensor,\ dry}/\overline{c}_{TEOM.dry}$ ratios for all sensors were 40%–50% lower than the values calculated at RH = 21% (Fig. S21). This result was consistent with previous studies in which correcting hourly ambient $PM_{2.5}$ concentrations reported by PurpleAir monitors using an approach similar to Equation (7) led to underestimation of hourly ambient $PM_{2.5}$ concentrations reported by a beta attenuation monitor (Malings et al., 2020) and 72-h ambient $PM_{2.5}$ concentrations derived from filter samples (Tryner et al., 2020). In some field studies, better results were obtained by applying a linear RH correction to data from Plantower PMS sensors (Malings et al., 2020; Zusman et al., 2020).

3.4. Comparison of sensor- and APS-Reported particle number concentrations

The Plantower PMS5003 underestimated number concentrations of 0.3–0.5 and 0.5–1.0 μm particles, relative to the corrected APS data, for all five aerosols tested during Experiments 1 and 2 (Fig. 4). The PMS5003 overestimated concentrations of 2.5–5.0 and 5.0–10 μm particles for all four aerosols tested during Experiment 1. The APS measured *very* low concentrations (<1 cm^{-3}) of 2.5–5.0 and 5.0–10 μm particles for these four aerosols (Fig. S22). Overall, the PMS5003 reported total number concentrations of particles between 0.3 and 10 μm that were 18%–35% of number concentrations derived from APS data spanning the same size range.

The Sensirion SPS30 overestimated the number concentrations of 2.5–4.0 and 4.0–10 μm particles, relative to the corrected APS data, for the four aerosols tested during Experiment 1. For all five aerosols tested during Experiments 1 and 2, the SPS30 reported total number concentrations of particles between 0.3 and 10 μm that were 104%–132% of number concentrations derived from APS data spanning the same size range. The best agreement between SPS30- and APS-reported particle counts in the 2.5–4.0 and 4.0–10 μm sizes ranges was observed for oil mist. Compared to the aerosols tested during Experiment 1, the oil mist contained more particles larger than 2.5 μm (Fig. S22).

3.5. Comparison of sensor- and APS-Reported particle number and mass distributions

The PMS5003 reported a surprisingly similar particle number size distribution for all of the aerosols measured during this study. The fraction of particles assigned to each size bin by sensors measuring 0.1, 0.27, 0.72, and 2 μm polystyrene latex spheres is shown in Fig. 5. The fraction of particles assigned to each size bin by sensors measuring ammonium sulfate, Arizona road dust, NIST Urban PM, wood smoke, and oil mist is shown in Fig. S24. The PMS5003 consistently reported that ~70% of particles were 0.3–0.5 μm. Our results support earlier hypotheses that particle number size distributions reported by Plantower PMS sensors are constrained by an algorithm and not free to assume any shape (He et al., 2020; Kelly et al., 2017). We compare our results for 0.1, 0.27, 0.72, and 2 μm PSL to those reported by Levy Zamora et al. (2019) for PMSA003 sensors in SI Section S2.5.

The size distribution reported by the Sensirion SPS30 did shift as the PSL size increased, but did not agree with corrected APS data for 0.72 or 2.0 μm PSL (Fig. 5). When measuring 0.1 or 0.27 μm PSL, the SPS30 reported that most particles were between 0.3 and 0.5 μm, while the APS reported that most particles were <0.5 μm. When measuring 0.72 μm PSL, the SPS30 and APS both reported that most particles were between 0.5 and 1.0 μm, but the SPS30 also reported that ~20% of particles were between 1.0 and 2.5 μm. When measuring 2.0 μm PSL, the SPS30 still reported that most particles were between 0.5 and 1.0 μm, while the APS correctly reported that most particles were between 1.0 and 2.5 μm. Similarly, the SPS30-reported size distribution for oil mist was shifted towards the right—relative to the size distributions reported for ammonium sulfate, nebulized Arizona road dust, NIST Urban PM, and wood

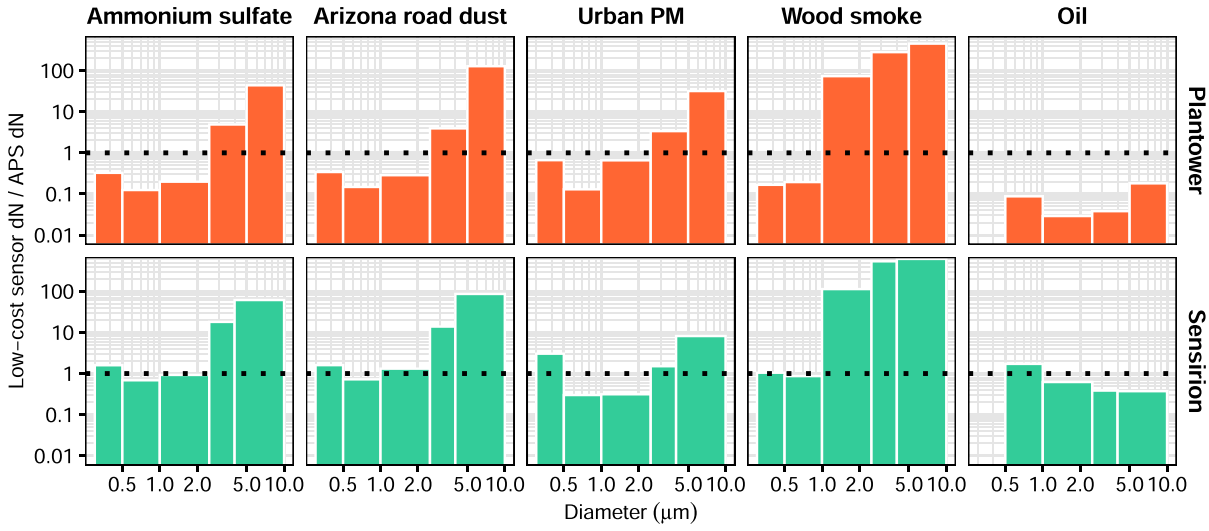

Fig. 4. Ratio of particle number concentration reported in each low-cost sensor size bin to the concentration derived from corrected APS data spanning the same size range. The data shown were recorded when the $PM_{2.5}$ concentration of each aerosol was between approximately 40 to 60 μg m^{-3} and the RH in the chamber was below 50%.

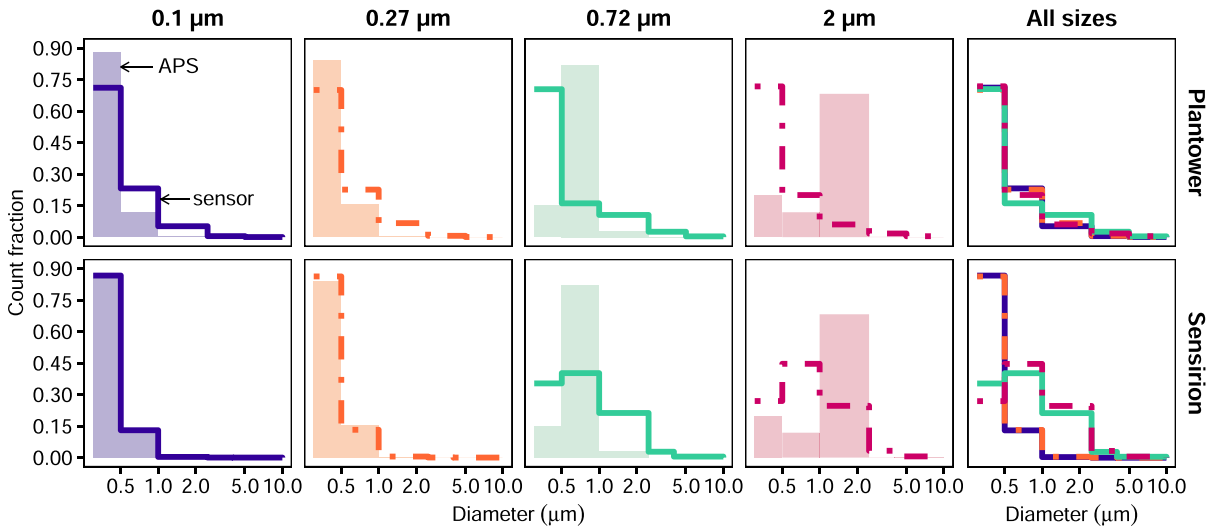

Fig. 5. Left four panels: Comparison of the fraction of particles assigned to each size bin by the low-cost sensors (lines) and the APS (rectangles) when measuring 0.10, 0.27, 0.72, and 2.0 µm PSL, respectively. Right panel: Comparison of the fraction of particles assigned to each size bin by Plantower PMS5003 and Sensirion SPS30 sensors for all four PSL sizes.

smoke—but did not agree with corrected APS data. The SPS30 and APS did assign similar fractions of particles to each size bin for Arizona road dust aerosolized using the fluidized bed generator (Fig. S24).

Particle number size distributions derived from corrected SMPS and APS data for each PSL size are shown in Fig. S25. The particle number size distribution measured during the background sample in which the nebulizer was on but contained only deionized water (i.e., no PSL) is shown in Fig. S26. In the worst case, the $dN/dlog(D_p)$ value calculated for the SPS30 0.3–0.5 µm size bin during the background sample with the nebulizer on was 28% of the $dN/dlog(D_p)$ value calculated for the same size bin when the SPS30 measured 2 µm PSL.

The fraction of PM mass assigned to each bin by the low-cost sensors when measuring polystyrene latex spheres is shown in Fig. 6. For all three sensors, the mass distribution shifted towards larger particle sizes as the known particle size increased. When measuring 0.27 µm PSL, both the SM-UART-04L and SPS30 sensors reported that almost all of the mass fell in the PM_1 bin. These results suggest that the sensors do use measurement data to allocate the measured aerosol to different mass fractions (e.g., PM_1, $PM_{2.5}$, PM_4, and PM_{10}).

For reference, the fraction of PM mass assigned to each mass bin by the APS is also shown in Fig. 6. When measuring 0.1 and 0.27 µm PSL, the SM-UART-04L and SPS30 did a better job than the APS of assigning all of the mass to the PM_1 bin. These particles were technically below the ~0.3 µm detection limit for the APS and the low-cost sensors. When measuring the 0.72 and 2.0 µm PSL, the APS did a better job than the low-cost sensors of assigning particle mass to the correct bin: the APS assigned most of the mass to the PM_1 bin when measuring 0.72 µm PSL and assigned all of the mass to the $PM_{2.5}$–PM_1 bin when measuring 2.0 µm PSL.

In Fig. 6, the fraction of PM mass in each bin as determined from the sensor-reported PM_1, $PM_{2.5}$, PM_4, and PM_{10} mass concentration data is compared to the fraction of PM mass in each bin as calculated from the particle count data (assuming that all particle sizes had the same density). For the PMS5003 and SPS30 sensors, there were discrepancies between the mass distributions obtained from the PM mass concentration data versus the particle count data for all four PSL sizes. It is sometimes assumed that particle count data are the "raw" values from which sensor-reported mass concentrations are calculated; however, our results suggest that sensor-reported particle number and mass concentrations are not consistent. An alternative explanation is that the relationship between the sensor-reported particle number and mass concentrations assumes different weights for different particle sizes (Lattanzio, 2020).

3.6. Sensor response after simulating extended use in a high-concentration environment

NIST Urban PM concentrations reported by the low-cost sensors and the TEOM during each evaluation conducted as part of Experiment 4 are shown in Fig. 7. Results obtained before the sensors were exposed to Arizona road dust aerosol from the fluidized bed generator were similar to those shown in Fig. 1. After six hours of exposure to Arizona road dust, one PMS5003 reported erroneously high NIST Urban PM concentrations (presumably because it became contaminated with Arizona road dust). After 18 h of exposure to Arizona road dust, three of the eight PMS5003 and two of the seven SM-UART-04L sensors reported erroneously high concentrations. Although some PMS5003 and SM-UART-04L sensors "failed" in this manner, the median response of all three sensor types remained similar for the duration of the experiment.

The precision of the $PM_{2.5}$ concentrations reported by all seven or eight sensors of each type when exposed to a NIST Urban Particulate Matter $PM_{2.5}$ concentration of approximately 30 µg m^{-3} (as measured by the TEOM) is illustrated in Fig. 8. In Fig. 8, a higher value of 0.75(IQR)/median represents lower precision. The precision of $PM_{2.5}$ "CF=1" values reported by PMS5003 sensors

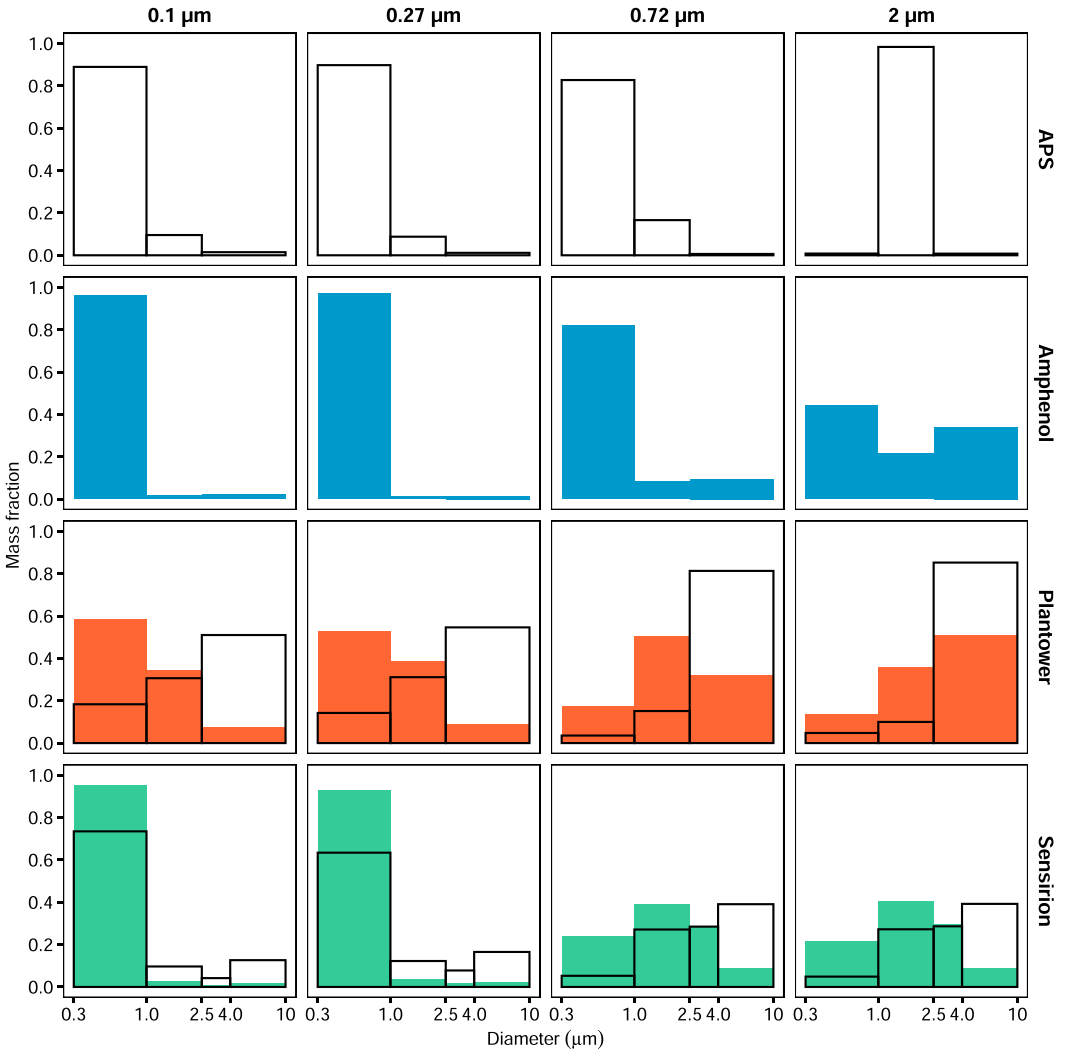

Fig. 6. Fraction of PM mass assigned to each bin by the APS and the low-cost sensors during tests with 0.10, 0.27, 0.72, and 2.0 µm PSL, respectively. Filled rectangles represent mass fractions calculated from the PM_1, $PM_{2.5}$, PM_4, and PM_{10} mass concentrations reported by the low-cost sensors. Unfilled rectangles represent mass fractions calculated from the particle count data reported by the APS, Plantower PMS5003, and Sensirion SPS30, respectively. The Amphenol SM-UART-04L did not report particle count data.

decreased continuously after six hours of exposure to Arizona road dust (results were similar for "atmospheric" values). The precision of $PM_{2.5}$ "standard smoke" values reported by SM-UART-04L sensors decreased continuously after nine hours of exposure (results were similar for "environment" values). By comparison, the precision of $PM_{2.5}$ values reported by SPS30 sensors remained relatively constant for the duration of the experiment.

The Sensirion SPS30 includes two features that are designed to prevent the sensor from becoming contaminated with PM: (1) filtered sheath air flows over the light detector continuously during operation, and (2) the sensor periodically undergoes a self-cleaning procedure in which the fan is accelerated to its maximum speed for 10 s in an effort to clear particles out of the sensing zone (Sensirion, 2020). The results shown in Fig. 8 indicate that SPS30 sensors were indeed more resistant to contamination than PMS5003 or SM-UART-04L sensors—potentially as a result of the aforementioned features.

During Experiment 4, we exposed the sensors to time-integrated Arizona road dust $PM_{2.5}$ and total PM concentrations (133 and 604 mg m^{-3} h, respectively) that were designed to be equivalent to exposing the low-cost sensors to 15 µg m^{-3} of $PM_{2.5}$ and 70 µg m^{-3} of total PM for approximately one year; however, it's possible that sensor degradation would have been less severe if the PMS5003 or SM-UART-04L sensors had been exposed to lower concentrations for a longer duration. For comparison, Sayahi et al. (2019) deployed two Plantower PMS1003 sensors and two PMS5003 sensors outdoors in Salt Lake City, UT, USA for a 320-day period when 24-h average $PM_{2.5}$ and PM_{10} concentrations ranged from 1.1 to 59.2 µg m^{-3} and 3.0–79.0 µg m^{-3}, respectively. One-third of the way through their deployment, one PMS1003 began to report erroneously high PM concentrations and continued to do so for the remainder of the study; however, the other three sensors did not exhibit this behavior (Sayahi et al., 2019).

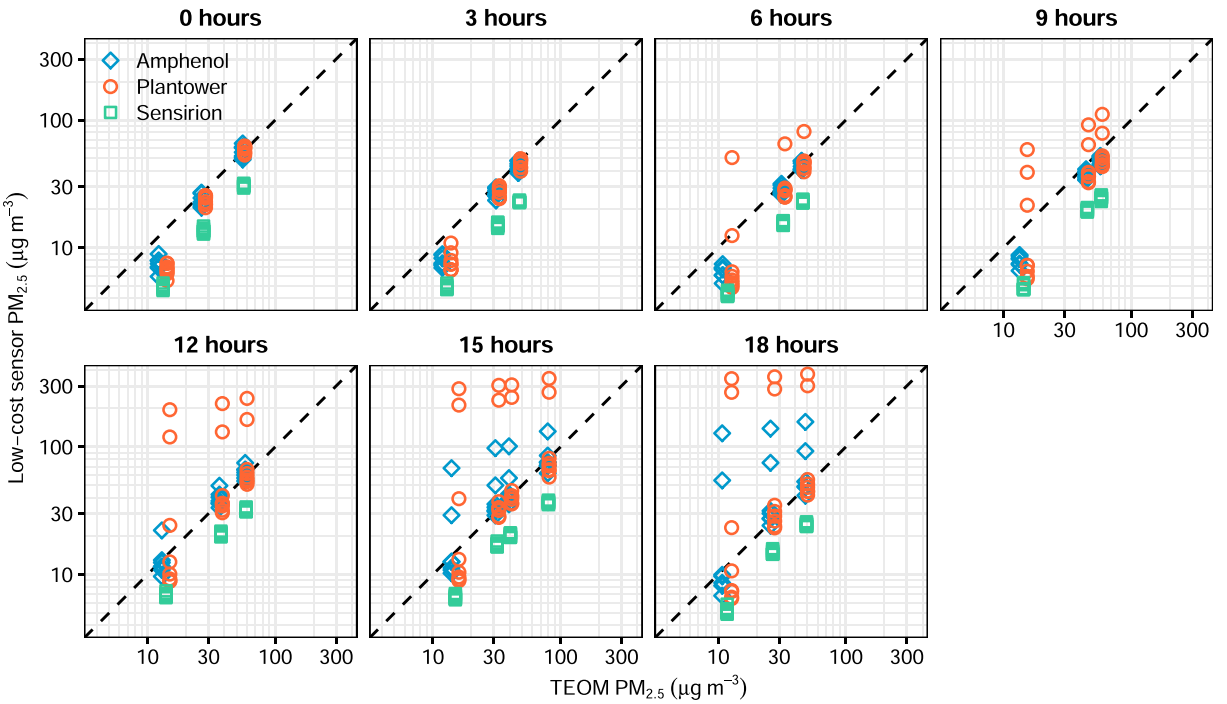

Fig. 7. NIST Urban PM concentrations reported by Plantower PMS5003 ("CF=1" values), Sensirion SPS30, and Amphenol SM-UART-04L ("standard smoke" values) sensors, compared to TEOM-reported $PM_{2.5}$ concentrations, during Experiment 4. A separate marker is shown for each of the seven or eight sensors of a given model. Plot titles indicate the number of hours for which the sensors were exposed to Arizona road dust before the data were collected.

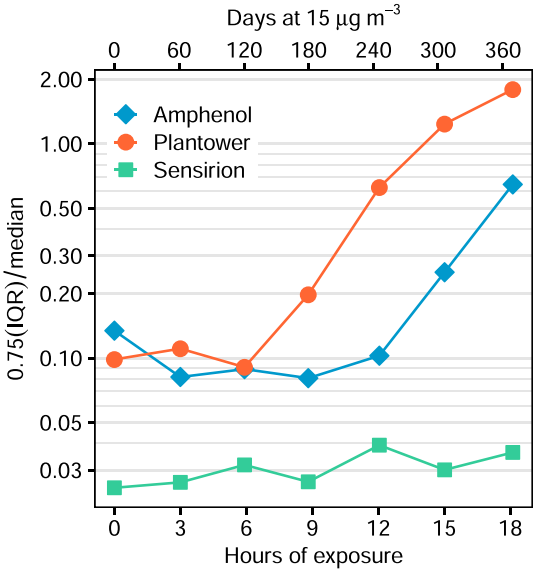

Fig. 8. Precision of $PM_{2.5}$ concentrations reported by seven or eight collocated Plantower PMS5003 ("CF=1" values), Sensirion SPS30, and Amphenol SM-UART-04L ("standard smoke" values) sensors when measuring a NIST Urban Particulate Matter $PM_{2.5}$ concentration of ~30 µg m^{-3} during each evaluation conducted as part of Experiment 4.

In addition to contamination with particles, extreme environmental conditions (e.g., high temperatures, excessive moisture) might also contribute to sensor degradation over time during outdoor use. The experiments described here were not designed to investigate these effects; all tests were conducted at room temperature and most were conducted in a low-RH environment.

4. Conclusions

We conducted laboratory experiments to evaluate the performance of three particulate matter sensors that cost less than $50 each: the Plantower PMS5003, Sensirion SPS30, and Amphenol SM-UART-04L. First, we investigated whether the sensors responded linearly to increasing $PM_{2.5}$ concentrations. Linear models explained $\geq$97% of the variance in PMS5003-reported ("CF=1" values) and SPS30-reported $PM_{2.5}$ concentrations, relative to TEOM-reported $PM_{2.5}$ concentrations, for ammonium sulfate concentrations up to 1025 μg m^{-3}, nebulized Arizona road dust concentrations up to 540 μg m^{-3}, and NIST Urban PM concentrations up to 330 μg m^{-3}; however, an F-test identified a significant ($\alpha = 0.05$) lack of fit between the model and the data for each sensor/aerosol combination. When exposed to wood smoke, all three sensors exhibited nonlinear responses that might have resulted from variations in the particle number size distribution during that test or error in the TEOM data. The SM-UART-04L did not report $PM_{2.5}$ concentrations >999 μg m^{-3}.

Second, we investigated how the relationship between the filter-derived $PM_{2.5}$ concentration and the time-averaged sensor-reported $PM_{2.5}$ concentration varied with aerosol type. The ratios of filter-derived to PMS5003-reported $PM_{2.5}$ concentrations were 1.4, 1.7, 1.0, 0.4, and 4.3 for ammonium sulfate, nebulized Arizona road dust, NIST Urban PM, wood smoke, and oil mist, respectively. The PMS5003 response was consistent with the amount of perpendicular-polarized light that Mie theory predicted would be scattered at 90° for each aerosol except oil mist. The SPS30 reported lower $PM_{2.5}$ concentrations than the PMS5003 for ammonium sulfate (filter-to-SPS30 ratio = 1.6), nebulized Arizona road dust (2.1), NIST Urban PM (2.1), and wood smoke (0.6). The SPS30 reported higher $PM_{2.5}$ concentrations than the PMS5003 for oil mist (filter-to-SPS30 ratio = 2.2) and Arizona road dust from the fluidized bed generator. Overall, these results suggested that there were differences in how the PMS5003 and SPS30 measured/interpreted light-scattering data.

Third, we investigated how precision varied between sensor models. SPS30 sensors were more precise than PMS5003 sensors when measuring ammonium sulfate, nebulized Arizona road dust, NIST Urban PM, oil mist, or PSL. The precision of all three sensor models decreased as PSL size increased—suggesting that particle size influenced precision.

Fourth, we investigated how sensor readings were affected by high relative humidity. Ammonium sulfate $PM_{2.5}$ concentrations reported by all three sensors increased, relative to TEOM-reported concentrations, as RH increased from 21% to 90%; however, correcting the low-cost sensor data using κ-Köhler theory led to underestimation of the dry, TEOM-reported $PM_{2.5}$ concentration at RH > 60%. Oil mist $PM_{2.5}$ concentrations reported by the low-cost sensors did not increase, relative to TEOM-reported $PM_{2.5}$ concentrations, as RH increased from 15% to 89%.

Fifth, we investigated whether particle count data reported by the low-cost sensors agreed with corrected APS data. Our results indicated that particle count data reported by the PMS5003 were not reliable. When measuring ammonium sulfate, nebulized Arizona road dust, NIST Urban PM, wood smoke, or oil mist, the PMS5003 reported total concentrations of 0.3–10 μm particles that were $\leq$35% of those derived from corrected APS data. Additionally, the PMS5003 reported a similar particle number size distribution for all of these aerosols as well as Arizona road dust aerosolized using a fluidized bed generator, 0.1 μm PSL, 0.27 μm PSL, 0.72 μm PSL, and 2.0 μm PSL. Particle count data reported by the SPS30 were somewhat more reliable. When measuring ammonium sulfate, nebulized Arizona road dust, NIST Urban PM, or oil mist, the SPS30 reported total concentrations of 0.3–10 μm particles that were 100%–130% of those derived from corrected APS data. The size distribution reported by the SPS30 shifted depending on the aerosol being measured, but the fractions of particles reported by the SPS30 in five size bins between 0.3 and 10 μm did not agree with corrected APS data for 0.72 μm PSL, 2.0 μm PSL, ammonium sulfate, nebulized Arizona road dust, NIST Urban PM, wood smoke, or oil mist.

Sixth, we investigated whether the sensors' assignments of PM to various size fractions (e.g., PM_1, $PM_{2.5}$, PM_{10}) agreed with APS data. For all three sensor models, the fraction of PM mass reported as PM_1, $PM_{2.5}$, and PM_{10} shifted as the PSL size increased from 0.1 to 2.0 μm, but the fraction of mass assigned to each size range typically did not agree with corrected APS data.

Seventh, we investigated whether sensor responses drifted over time in a high-concentration environment. After we exposed the sensors to time-averaged Arizona road dust $PM_{2.5}$ and total PM concentrations of 7300 μg m^{-3} and 33,000 μg m^{-3} during for 18 h, three of eight PMS5003 sensors and two of seven SM-UART-04L sensors reported erroneously high $PM_{2.5}$ concentrations. The SPS30 sensors retained their precision over the duration of this experiment—suggesting that their sheath air flow and automatic cleaning features might indeed protect them from contamination during extended use in a high-concentration environment.

Declaration of competing interest

John Volckens is a scientific founder of Access Sensor Technologies, LLC and has an equity interest in the company. The terms of this arrangement have been reviewed and approved by Colorado State University in accordance with its conflict of interest policies. Additionally, Jessica Tryner is a part-time employee of Access Sensor Technologies. This arrangement has been disclosed to Colorado State University. Access Sensor Technologies has no financial relationship with the manufacturers of the low-cost particulate matter sensors evaluated in this study. Furthermore, the results presented herein should not be interpreted as an endorsement of any particular low-cost particulate matter sensor.

Acknowledgements

The authors thank Sai Gowdar and Casey Quinn for developing the firmware and software used to acquire data from the low-cost sensors.

Appendix A. Supplementary data

Supplementary data to this article can be found online at https://doi.org/10.1016/j.jaerosci.2020.105654.

Funding

This work was supported by the National Institute for Occupational Safety and Health within the US Centers for Disease Control [grant numbers OH010635 and OH010662]. The content is solely the responsibility of the authors and does not necessarily represent the official views of the Centers for Disease Control or the National Institute for Occupational Safety and Health.

Data availability

Data related to this article are available through the open access repository service Mountain Scholar: https://hdl.handle.net/10217/207239 (Tryner, Mehaffy, Miller-Lionberg, & Volckens, 2020).

References

Analytical Methods Committee. (1994). Is my calibration linear? *The Analyst, 119*(11), 2363–2366. https://doi.org/10.1039/an9941902363.

Amphenol Advanced Sensors. (2019). *SM-UART-04L PM2.5 + PM10 particulate dust sensor*. https://amphenol-sensors.com/en/component/edocman/514-telaire-sm-uart-04l-laser-dust-sensor-application-note/download?Itemid=8488%20%27. (Accessed 28 November 2019).

Anderson, J. O., Thundiyil, J. G., & Stolbach, A. (2012). Clearing the air: A review of the effects of particulate matter air pollution on human health. *Journal of Medical Toxicology, 8*(2), 166–175. https://doi.org/10.1007/s13181-011-0203-1.

Arachchige, C. N. P. G., Prendergast, L. A., & Staudte, R. G. (2019). *Robust analogues to the coefficient of variation*. https://arxiv.org/abs/1907.01110v1.

Austen, K. (2015). Environmental science: Pollution patrol. *Nature, 517*(7533), 136–138. https://doi.org/10.1038/517136a.

Brauer, M., Freedman, G., Frostad, J., van Donkelaar, A., Martin, R. V., Dentener, F., et al. (2016). Ambient air pollution exposure estimation for the global burden of disease 2013. *Environmental Science & Technology, 50*(1), 79–88. https://doi.org/10.1021/acs.est.5b03709.

Bulot, F. M. J., Johnston, S. J., Basford, P. J., Easton, N. H. C., Apetroaie-Cristea, M., Foster, G. L., et al. (2019). Long-term field comparison of multiple low-cost particulate matter sensors in an outdoor urban environment. *Scientific Reports, 9*(1), 7497. https://doi.org/10.1038/s41598-019-43716-3.

Camalier, L., Eberly, S., Miller, J., & Papp, M. (2007). *Guideline on the meaning and the use of precision and bias data required by 40 CFR Part 58 Appendix A* (EPA-454/B-07-001). U.S. Environmental Protection Agency https://www3.epa.gov/ttn/amtic/files/ambient/qaqc/PBGuidance101007.pdf.

Crilley, L. R., Shaw, M., Pound, R., Kramer, L. J., Price, R., Young, S., et al. (2018). Evaluation of a low-cost optical particle counter (Alphasense OPC-N2) for ambient air monitoring. *Atmospheric Measurement Techniques, 11*(2), 709–720. https://doi.org/10.5194/amt-11-709-2018.

DeCarlo, P. F., Slowik, J. G., Worsnop, D. R., Davidovits, P., & Jimenez, J. L. (2004). Particle morphology and density characterization by combined mobility and aerodynamic diameter measurements. Part 1: Theory. *Aerosol Science and Technology, 38*(12), 1185–1205. https://doi.org/10.1080/027868290903907.

Delp, W. W., & Singer, B. C. (2020). Wildfire smoke adjustment factors for low-cost and professional PM2.5 monitors with optical sensors. *Sensors, 20*(13), 3683. https://doi.org/10.3390/s20133683.

Farmer, D. K., Vance, M. E., Abbatt, J. P. D., Abeleira, A., Alves, M. R., Arata, C., et al. (2019). Overview of HOMEChem: House observations of microbial and environmental chemistry. *Environmental Sciences: Processes & Impacts, 21*(8), 1280–1300. https://doi.org/10.1039/C9EM00228F.

Gonzalez, C. A., & Watters, R. L., Jr. (2015). *Certificate of analysis: Standard reference material 1648a urban particulate matter*. National Institute of Standards and Technology. https://www-s.nist.gov/srmors/certificates/1648A.pdf.

Hagan, D. H., & Kroll, J. H. (2020). Assessing the accuracy of low-cost optical particle sensors using a physics-based approach. *Atmos. Meas. Tech. Discuss.*. https://doi.org/10.5194/amt-2020-188. in review.

He, M., Kuerbanjiang, N., & Dhaniyala, S. (2020). Performance characteristics of the low-cost Plantower PMS optical sensor. *Aerosol Science and Technology, 54*(2), 232–241. https://doi.org/10.1080/02786826.2019.1696015.

IHME. (2018). *GBD compare*. Institute for Health Metrics and Evaluation. https://vizhub.healthdata.org/gbd-compare/.

Jayaratne, R., Liu, X., Thai, P., Dunbabin, M., & Morawska, L. (2018). The influence of humidity on the performance of a low-cost air particle mass sensor and the effect of atmospheric fog. *Atmospheric Measurement Techniques, 11*(8), 4883–4890. https://doi.org/10.5194/amt-11-4883-2018.

Kelly, K. E., Whitaker, J., Petty, A., Widmer, C., Dybwad, A., Sleeth, D., et al. (2017). Ambient and laboratory evaluation of a low-cost particulate matter sensor. *Environmental Pollution, 221*, 491–500. https://doi.org/10.1016/j.envpol.2016.12.039.

Kreidenweis, S. M., & Asa-Awuku, A. (2014). Aerosol hygroscopicity: Particle water content and its role in atmospheric processes. In Ralph Keeling, & Lynn Russell (Eds.) (2nd,, *5. Treatise on Geochemistry* (pp. 331–361). Elsevier. https://doi.org/10.1016/B978-0-08-095975-7.00418-6.

Kuula, J., Mäkelä, T., Aurela, M., Teinilä, K., Varjonen, S., González, Ó., et al. (2020). Laboratory evaluation of particle-size selectivity of optical low-cost particulate matter sensors. *Atmospheric Measurement Techniques, 13*(5), 2413–2423. https://doi.org/10.5194/amt-13-2413-2020.

Lattanzio, L. (2020). *Particulate matter sensing for air quality measurements*. Sensirion. Retrieved April 13, 2020 https://www.sensirion.com/en/about-us/newsroom/sensirion-specialist-articles/particulate-matter-sensing-for-air-quality-measurements/.

Levy Zamora, M., Xiong, F., Gentner, D., Kerkez, B., Kohrman-Glaser, J., & Koehler, K. (2019). Field and laboratory evaluations of the low-cost Plantower particulate matter sensor. *Environmental Science & Technology, 53*(2), 838–849. https://doi.org/10.1021/acs.est.8b05174.

Magi, B. I., Cupini, C., Francis, J., Green, M., & Hauser, C. (2019). Evaluation of PM2.5 measured in an urban setting using a low-cost optical particle counter and a Federal Equivalent Method Beta Attenuation Monitor. *Aerosol Science and Technology, 54*(2), 147–159. https://doi.org/10.1080/02786826.2019.1619915.

Malings, C., Tanzer, R., Hauryliuk, A., Saha, P. K., Robinson, A. L., Presto, A. A., et al. (2020). Fine particle mass monitoring with low-cost sensors: Corrections and long-term performance evaluation. *Aerosol Science and Technology, 54*(2), 160–174. https://doi.org/10.1080/02786826.2019.1623863.

Petters, M. D., & Kreidenweis, S. M. (2007). A single parameter representation of hygroscopic growth and cloud condensation nucleus activity. *Atmospheric Chemistry and Physics, 7*(8), 1961–1971. https://doi.org/10.5194/acp-7-1961-2007.

Pillarisetti, A., Carter, E., Rajkumar, S., Young, B. N., Benka-Coker, M. L., Peel, J. L., et al. (2019). Measuring personal exposure to fine particulate matter (PM2.5) among rural Honduran women: A field evaluation of the Ultrasonic Personal Aerosol Sampler (UPAS). *Environment International, 123*, 50–53. https://doi.org/10.1016/j.envint.2018.11.014.

Sayahi, T., Butterfield, A., & Kelly, K. E. (2019). Long-term field evaluation of the Plantower PMS low-cost particulate matter sensors. *Environmental Pollution, 245*, 932–940. https://doi.org/10.1016/j.envpol.2018.11.065.

Sensirion. (2020). *Datasheet SPS30: Particulate matter sensor for air quality monitoring and control*. https://www.sensirion.com/fileadmin/user_upload/customers/sensirion/Dokumente/9.6_Particulate_Matter/Datasheets/Sensirion_PM_Sensors_SPS30_Datasheet.pdf.

Singer, B. C., & Delp, W. W. (2018). Response of consumer and research grade indoor air quality monitors to residential sources of fine particles. *Indoor Air, 28*(4), 624–639. https://doi.org/10.1111/ina.12463.

Sousan, S., Koehler, K., Hallett, L., & Peters, T. M. (2017). Evaluation of consumer monitors to measure particulate matter. *Journal of Aerosol Science, 107*, 123–133. https://doi.org/10.1016/j.jaerosci.2017.02.013.

Sumlin, B. J. (2020). *Online user's guide for the Python Mie Scattering package (PyMieScatt)*. https://pymiescatt.readthedocs.io/en/latest/.

Sumlin, B. J., Heinson, W. R., & Chakrabarty, R. K. (2018). Retrieving the aerosol complex refractive index using PyMieScatt: A Mie computational package with visualization capabilities. *Journal of Quantitative Spectroscopy and Radiative Transfer, 205*, 127–134. https://doi.org/10.1016/j.jqsrt.2017.10.012.

Toren, K., Bergdahl, I. A., Nilsson, T., & Jarvholm, B. (2007). Occupational exposure to particulate air pollution and mortality due to ischaemic heart disease and cerebrovascular disease. *Occupational and Environmental Medicine, 64*(8), 515–519. https://doi.org/10.1136/oem.2006.029488.

Tryner, J., L'Orange, C., Mehaffy, J., Miller-Lionberg, D., Hofstetter, J. C., Wilson, A., et al. (2020). Laboratory evaluation of low-cost PurpleAir PM monitors and in-field correction using co-located portable filter samplers. *Atmospheric Environment, 220*, Article 117067. https://doi.org/10.1016/j.atmosenv.2019.117067.

Tryner, J., Mehaffy, J., Miller-Lionberg, D., & Volckens, J. (2020). *Dataset associated with "Effects of aerosol type and simulated aging on performance of low-cost PM sensors"*. https://hdl.handle.net/10217/207239.

Tryner, J., Quinn, C., Windom, B. C., & Volckens, J. (2019). Design and evaluation of a portable $PM_{2.5}$ monitor featuring a low-cost sensor in line with an active filter sampler. *Environmental Sciences: Processes & Impacts, 21*(8), 1403–1415. https://doi.org/10.1039/C9EM00234K.

Volckens, J., & Peters, T. M. (2005). Counting and particle transmission efficiency of the aerodynamic particle sizer. *Journal of Aerosol Science, 36*(12), 1400–1408. https://doi.org/10.1016/j.jaerosci.2005.03.009.

Wang, Y., Li, J., Jing, H., Zhang, Q., Jiang, J., & Biswas, P. (2015). Laboratory evaluation and calibration of three low-cost particle sensors for particulate matter measurement. *Aerosol Science and Technology, 49*(11), 1063–1077. https://doi.org/10.1080/02786826.2015.1100710.

Yong, Z. (2016). *Digital universal particle concentration sensor: PMS5003 series data manual.* Plantower.

Zusman, M., Schumacher, C. S., Gassett, A. J., Spalt, E. W., Austin, E., Larson, T. V., et al. (2020). Calibration of low-cost particulate matter sensors: Model development for a multi-city epidemiological study. *Environment International, 134*, 105329. https://doi.org/10.1016/j.envint.2019.105329.